Journal of
Manufacturing and Materials Processing

MDPI

Article

Improved Use of the Full Length of Milling-Tool Flutes in Processes of Air-Contour Milling

César García-Hernández [1,2,*], Juan-Jesús Valdivia-Sánchez [3], Pedro Ubieto-Artur [1,2], Mariano García-Arbués [4], Anastasios Tzotzis [5], Juan-José Garde-Barace [3], Francisco Valdivia-Calvo [3] and José-Luis Huertas-Talón [2,6]

1 Department of Design and Manufacturing Engineering, University of Zaragoza, 50018 Zaragoza, Spain
2 Design for Safety (D4S), I3A, University of Zaragoza, 50018 Zaragoza, Spain
3 CPIFP "Corona de Aragón", 50009 Zaragoza, Spain
4 Marena, S.L., 50171 La Puebla de Alfindén, Spain
5 Department of Product and Systems Design Engineering, University of Western Macedonia, 50 150 Kozani, Greece
6 Regional Innovation Centre for Vocational Education and Training CIFPA Aragón, 50197 Zaragoza, Spain
* Correspondence: garcia-hernandez.cesar@unizar.es

Abstract: The cutting length of milling tools must be longer than the axial distance of the material to be processed. In fact, in most cases, the cutting length far exceeds the thickness of the material to be removed. Therefore, along the entire length of the milling-tool flutes, only the area farthest from the shank wears out, leaving the rest of the tool practically without any wear, especially in the area closest to the shank. This research analyses a toolpath model to use the complete length of the milling tool flutes, in those machining operations in which it is possible, with the objective of reducing the costs associated with tool wearing and resharpening. This improves the tool performance, which clearly increases the sustainability of the milling process. For this purpose, it is necessary to transform the numerical control programme that performs a flat (2D) toolpath into a helical (3D) one by decomposing the arcs and rectilinear segments into a succession of points within a precision range. A negative aspect of this method is that it can only be applied to bottomless contours in processes of air-contour milling.

Keywords: sustainable milling; toolpath; curve decomposition; 2D to 3D toolpath; helical application; CAM

Academic Editor: Steven Y. Liang

Received: 4 March 2025
Revised: 25 April 2025
Accepted: 27 April 2025
Published: 2 May 2025

Citation: García-Hernández, C.; Valdivia-Sánchez, J.-J.; Ubieto-Artur, P.; García-Arbués, M.; Tzotzis, A.; Garde-Barace, J.-J.; Valdivia-Calvo, F.; Huertas-Talón, J.-L. Improved Use of the Full Length of Milling-Tool Flutes in Processes of Air-Contour Milling. *J. Manuf. Mater. Process.* **2025**, *9*, 150. https://doi.org/10.3390/jmmp9050150

1. Introduction

The use of the full cutting length of milling tools has been previously studied for ball nose end mills in finishing operations, requiring at least four axes to be able to vary the axial angle with respect to the flat surface [1–3]. In [4], a 30° angle was used as an optimal solution in the experimental stage. In those cases, it is also necessary to adapt the rotation frequency of the spindle [5] by varying the contact radius between the flutes and the surface. When the surface is not flat, continuing with the ball nose end mill, the tilt angle depends on the normal to the surface (which varies by geometry) and the orientation of the cutter axis. To improve the tool wear, it is possible to act on both the angle of the ball nose meeting the surface and on the rotation speed to keep the cutting speed as constant as possible. This implies, as in the case of the flat surface, variation in the feed rate [6]. Another alternative, in the case of non-flat surfaces, is to modify the shape of the toolpaths, which has been proven to be positive in machines with only three axes [7], causing also changes in the acceleration of the milling head between the different toolpaths. For this purpose, it is

always necessary to increase or decrease the rotation frequency of the spindle, or on the contrary, to apply an acceleration–deceleration movement that causes the rapid warming of the braking resistances [8]. When machining sharp corners, strategies that allow a constant engagement angle [9] are applied. These strategies are extended to grooving, resulting in trochoidal milling, for which different alternatives have also been studied previously. Part of this research team studied the effect of varying the feed rate several years ago [10] and more recently [11]. There are also previous works in which researchers used sensors to determine the energy cost of the process [12]. The problem is that these types of processes cannot be carried out on older machines or those with fewer configuration options, unless the milling machines could be equipped with sensors, allowing them to work in an adaptive closed loop.

The development of strategies for the optimisation of the milling has been studied from the point of view of sustainability in manufacturing processes [13–15]. Different approaches could be mentioned, from optimising the tool design parameters thanks to high speed video recordings [16] to optimising the tilting angle in order to minimise machining-induced burr size, especially with end-of-life tools [17].

Although in this paper we only refer to contour milling, it should be considered that curves can be concave and convex, the "inner corner" being the most extreme case. The equations applied in our experimental stage are explained in Section 2.2, but when milling corners, it is better to use a progressive feed rate for the initial and final parts of the toolpath [18]. We will apply the method explained in [19], which is particularly relevant to spherical milling tools [20]. The referred equations can even be found in manufacturer catalogues [21], but we have considered it relevant to include them in this paper to ensure clarity.

The study described below (side milling when the end mill is not working on its front face) was inspired by the helical machining of holes [22]. Although it only applies to a trajectory for a linear test, it was also considered very interesting to study a context in which the tool describes an ascending and descending toolpath, according to a sinusoid [23], as referred to in Section 2. This could also be applied to our experimental study, although we decided to perform linear interpolations for any type of profiling toolpath, such as those presented in Figure 1.

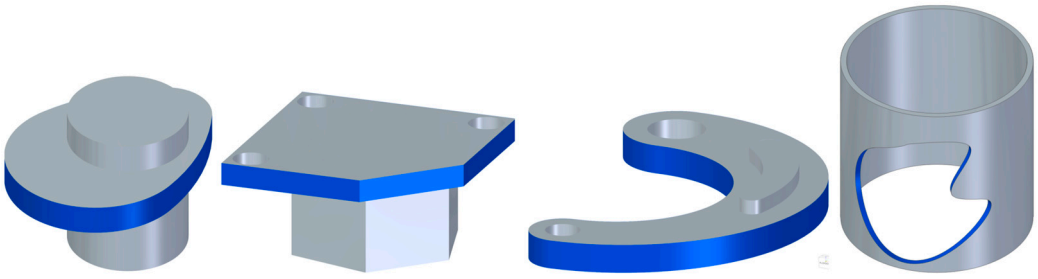

Figure 1. Examples of parts in which this study could be applied.

All the parts shown in Figure 1 have the common feature of a contour without a bottom, so the milling tool cuts only with its peripheral area, and not axially. For this reason, we termed this process "air-contour milling". When the part to be milled has a bottom, the projection on it defines the toolpath to be followed by the milling tool, but this is not the case here. Moreover, as shown below, the milling tool clearly goes under the contour of the workpiece.

When making a single part, as an improvement or for repair (not for series production), the only condition is that the milling tool must be a standard multi-purpose one. This is why the MA911 milling tool [21] was chosen, as discussed in Section 3.2. This standard

milling tool has a geometry similar to the one mentioned in [24]. The process of cutting edge preparation described in [25] is similar to the micro-rounding of the cutting edge employed by our milling tool. These features, combined with the selection of the trajectory as in [26,27], improve the milling process.

Finally, an important aspect is the smoothing of the toolpath, defined by a multitude of points whose final position is defined by G1 (straight lines). It is well known that the G5 function can generally perform this task, but there are more specialised methods available [28]. Some of these methods are implemented in numerical controls that include high-speed functions, for example [29]. Although the required syntax varies from one NC to another, the objective is the same—toolpath smoothing; for our purpose, G5 is good enough.

The method described below was developed for milling parts like the first three examples shown previously, requiring a two-dimensional toolpath, although this could also be generalised for the last one.

In this study, we optimised the use of full-length milling tool flutes, with the condition that the parts to be milled have no bottom (air-contour milling). To do this, the arcs and lines (which could be other curves) are decomposed into points which, through the use of smoothing functions, describe a continuous milling toolpath. In addition, it is possible to adapt the feed rate depending on whether the contour is concave or convex with respect to the tool. The method was applied to a real part, obtaining a uniform wear along the entire length of the milling tool.

2. Research Method

2.1. Geometry

In the contouring process using a milling tool (Figure 2), it is very common to use a standard end mill with a determined cutting length longer than the maximum thickness of the part to be cut, with it being possible to divide it into one or more steps. In any case, the flute length of the milling tool will only be used partially.

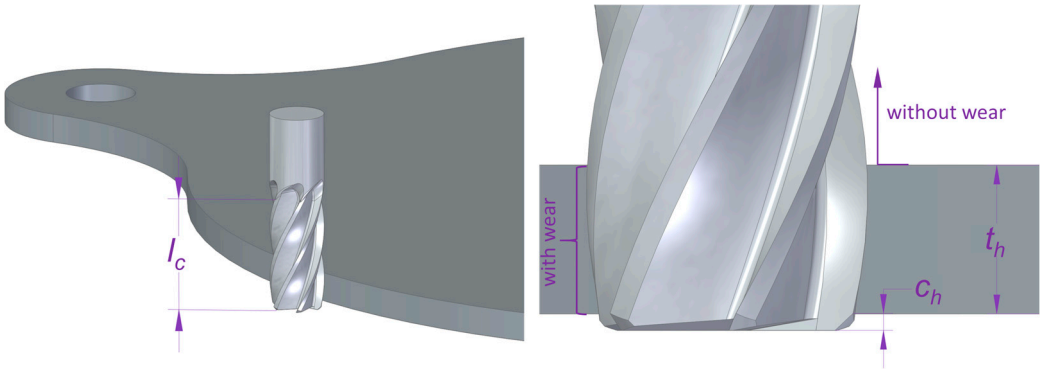

Figure 2. Contouring of a part.

However, in the case of external profiling, when the part to be milled has an open bottom, the milling tool must slightly exceed the lower limit of that bottom of the part. This is due to the shape of the edge of the milling tool tip, which can be either rounded or bevelled, in order to avoid strain concentration. For example, in a milling tool with four teeth and a 6 mm diameter, the typical edge chamfer or radius can be around 0.25 mm, depending on the diameter of the tool and the manufacturer's design parameters, so the tool catalogue must be consulted. For this reason, a distance at least equal to that radius must be kept below the milled part (Figure 2, right).

Sometimes, when the parts to be milled do not have an open bottom and the number of pieces to manufacture is big enough, it could be possible to manufacture, on request, milling tools with short flute lengths in both sides of the shank, as shown in Figure 3. Thus, the amount of material required for manufacturing the tool can be optimised by sharpening flutes in both sides, contributing to a more sustainable milling process.

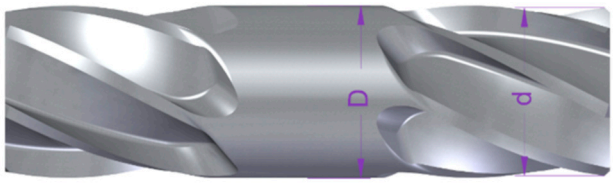

Figure 3. Milling tool with both sides sharpened.

On the other hand, in a machining workshop with a short run of parts, or even with a single part order, as in the case that has been considered with the proposed piece in this study, the milling tools are normally standard ones. The cutting length of these standard tools is, in some cases, much longer than the depth to be milled. Consequently, the cutting length of the tool is only partially worn. Although the rest of the cutting length is still perfectly sharp, the milling tool can become useless for precision works, due to its partially worn flutes, as shown in Figure 2.

In our case, the optimising solution that this research proposes is based on the use of almost the total cutting length of the tool during the milling process. For that purpose, it is proposed to start the machining process at the farthest area from the tool holder, to be ended with the nearest one (or vice versa). This means describing a helical milling toolpath with a decreasing (or increasing) vertical position (z value), as shown in Figure 4.

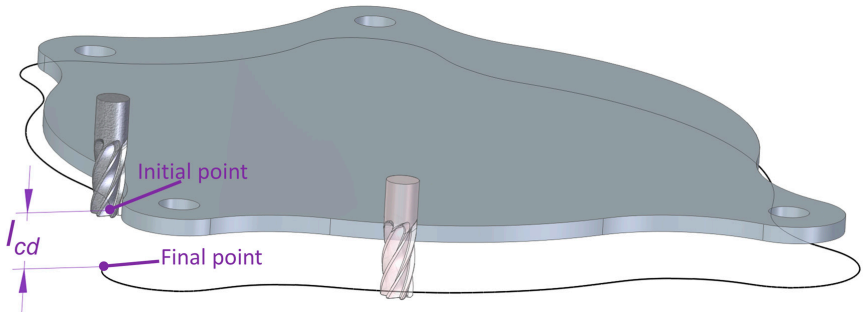

Figure 4. Helical milling toolpath with a decreasing vertical position of the tool.

Another alternative to the previous procedure could be to vertically move the tool, up and down, a certain number of times related to the milled distance (Figure 5). In this study, only the strategy previously described (and graphically shown in Figure 4) was considered.

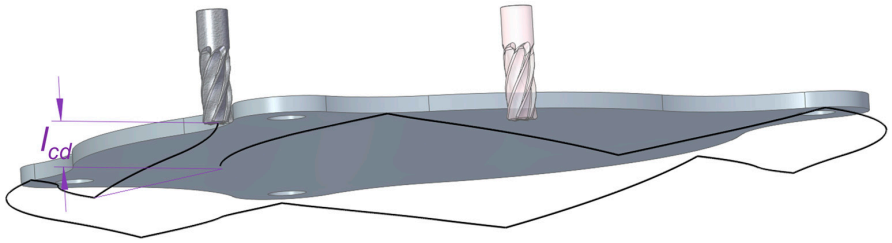

Figure 5. Milling tool vertically moved (up and down) along the profile.

It is important to point out that there are other suitable processes for this kind of works, such as water cutting, plasma, EDM, laser or electron beam cutting. Despite this,

milling can be considered a versatile process, which is affordable and can be developed in most machining workshops, and can even be employed with the manufacturer's resources.

In [23], a case is described in which the transition points describe a sinusoidal toolpath, although the milling follows a straight line. Choosing a sinusoidal or a different toolpath should not be a key aspect, and we decided to use a linear toolpath, which describes a helicoidal contour. Here, the key feature is the contact of the full length of the milling tool with the part's contour, increasing the service life of the tool and requiring less cutting force. When smoothing functions are applied (G5 in older machines and "look ahead" functions with higher speeds in newer ones), the obtained surface quality is increased. Figure 6 shows three different milling contours: without a smoothing function (a), with it (b), and describing an ascending and descending toolpath (c) with the milling tool (as shown in Figure 5). It can be appreciated that older machines describe a "bumpy" toolpath when having to accelerate and decelerate (without G5 function). In this study, we only compared a horizontal toolpath with a helicoidal one, using a smoothing function, thus obtaining the surface quality shown in Figure 6b.

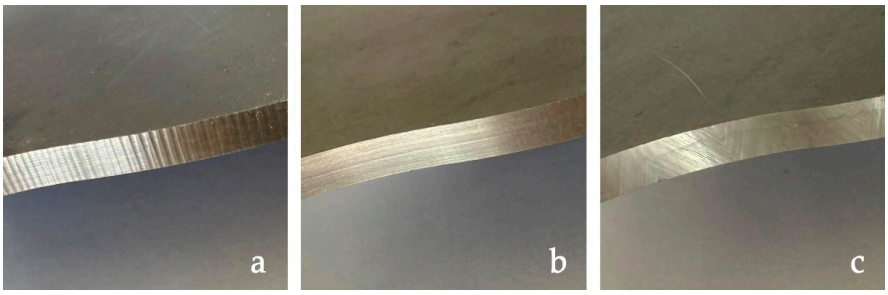

Figure 6. Contours without a smoothing function (**a**), with it (**b**), and describing an ascending and descending toolpath with the milling tool (**c**).

The contour achieved by the parts previously considered can be reached by a succession of curves of any type, although in this study it will be limited to straight lines and circumference arcs. Other types of curves can be decomposed into points, using each curve's radius around the point for the transformation.

Linear movements encounter no difficulty, since the spatial points keep the two coordinates (XY) that they would have in the plane, changing only the third one (Z). Usually, for this type of process, the XY plane is used. However, the cases of Figures 4 and 5 are different, and the linear displacement must also be decomposed into points to add the Z coordinates, as explained via the curves in the previous paragraph.

The third coordinate (Z) is related to the flute length of the milling tool. It depends on the linear segments in which the curve is decomposed, being related to the total perimeter, as will be detailed below for the arcs. The toolpath, shown in Figures 4 and 5, must be decomposed into adjacent points. This 2D toolpath decomposition process could be undertaken using the CAM system or using the method described below. In order to obtain the third coordinate (Z), the process explained in Section 2.4, in which the displacement of the milling tool along the Z axis is described, can be used.

The mathematical requirements are simple, as described in the previous paragraph, with this simplicity of the mathematical method being key to its real applicability. For example, the concept of proportionality is the basis for calculating the third coordinate and the new feed rate in the space, in addition to the modification of convex or concave curves.

2.2. New Feed Rate

If all toolpaths were straight, the flat (2D) trajectory would be shorter than the helical one. Therefore, to make the component of the feed rate on the plane the same, the feed rate

on the toolpath must be greater. It can be considered that, in order to calculate the total perimeter, the points of the final toolpath must be known, but this is not necessarily true (as shown in Figure 7). To go from one point to the next one, a straight line is followed (due to the real movements of the machine, they will be approximately rectilinear displacements), so it is possible to obtain the distance between each pair of points. In fact, this is not necessary, as the succession of straight segments conforms to the hypotenuse of a right triangle, in which one of its catheti has the length of the 2D perimeter and the other one is the displacement of the milling tool (Figure 7). This displacement of the milling tool gives the length of the available cut (l_{cd}), as shown in Equation (1), which can be deduced from Figures 2 and 4. Therefore, thanks to the Pythagorean Theorem, it is simple to calculate the displacement of the milling tool in 3D (as shown in Figure 7).

$$l_{cd} = l_c - t_h - c_h \tag{1}$$

where (as shown in Figure 2) l_c is the cutting length of the milling tool, t_h is the thickness of the part, and c_h is be the chamfer or the corner radius of the milling tool.

$$p_{3D} = \sqrt{{p_{2D}}^2 + {l_{cd}}^2} \tag{2}$$

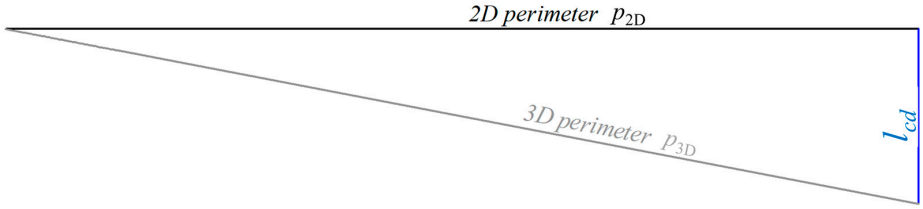

Figure 7. The time to cover both toolpaths must be the same.

According to Equation (2), the longer the perimeter and the shorter the cutting length of the milling tool, the more similar both perimeters will be.

In the cases shown in Figures 5 and 8, the concept of milling half-pitch is used. The pitch describes the complete "wave"—down and up. The experimental code was programmed so that, with the entrance half-pitch (p_h), the number of steps (n_s) was an integer within the 2D perimeter. This implies that the new half-pitch (p_h) was the 2D perimeter within the mentioned number of steps (n_s). Figure 8 shows the calculation of the 3D perimeter when the milling tool goes down or up n_s times.

$$n_s = ROUNDUP\left(\frac{p_{2D}}{p_h}, 0\right) \Rightarrow p_h = \frac{p_{2D}}{n_s} \tag{3}$$

$$p_{3D} = n_s\sqrt{{p_h}^2 + {l_{cd}}^2} \tag{4}$$

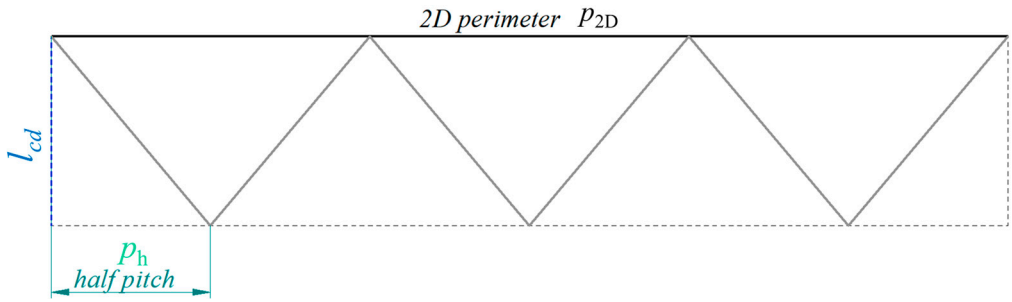

Figure 8. 3D perimeter with half-pitch.

It should be noted that the perimeter obtained with Equations (2) and (4) must be slightly bigger (especially in the case of Equation (4)) than the sum of all the distances between each pair of consecutive points into which the perimeter is divided, because each arc is being replaced by its chord.

As the time (t) to describe p_{3D} must be the same as the time required to describe p_{2D}, the obtained feed rate is

$$v_f = f_z \cdot z \cdot n \tag{5}$$

where f_z (mm/tooth) is the feed per tooth, z is the number of teeth in the milling tool and n is the spindle speed (rpm). The feed rate on 3 axes can be obtained with the equation

$$t = \frac{p_{2D}}{v_f} = \frac{p_{3D}}{v_{f3D}} \Rightarrow v_{f3D} = v_f \frac{p_{3D}}{p_{2D}} \tag{6}$$

This feed rate, at the same time, must be modified to cover an internal or external curvature toolpath of the cutter.

2.3. Correction of the Feed per Tooth According to Concavity

The feed rate of the milling tool (6) is only applicable to the rectilinear segments of the whole geometry. When a curved toolpath is machined, such as in our succession of circumference arcs, the feed rate must be corrected again (Figure 9).

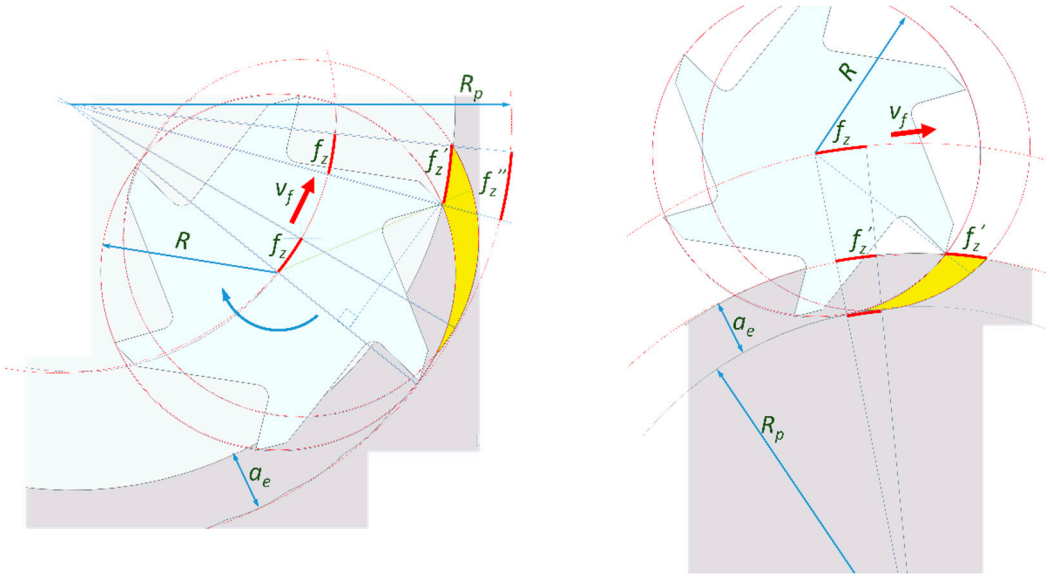

Figure 9. Correction of the feed per tooth according to concavity.

In both cases, the required time must be the same, but in Figure 9 (left), when the milling tool works inside, it can be observed that the feed per tooth (and therefore, the feed per tooth on the material surface) increases in relation to the feed rate in the centre of the tool, according to Equation (5). In Figure 9 (right), the opposite can be observed,

$$t = \frac{f_z''}{\omega \cdot R_p} = \frac{f_z}{\omega \cdot (R_p - R)} \Rightarrow f_z = \frac{R_p - R}{R} f_z'' \tag{7}$$

$$t = \frac{f_z''}{\omega \cdot R_p} = \frac{f_z}{\omega \cdot (R_p + R)} \Rightarrow f_z = \frac{R_p + R}{R} f_z'' \tag{8}$$

where R_p is the radius of the section being milled, R is the radius of the milling tool, f_z is the feed per tooth to be used for programming (5) and f_z'' is the feed per tooth that the tool manufacturer recommends.

2.4. Displacement of the Milling Tool Along the Z Axis

As previously explained, the aim is to apply the proportional distribution criterion. For every displacement in the XY plane, Δl, a vertically descending movement of the milling tool will be described, as

$$\Delta z = \frac{l_{cd}}{p_{2D}/n_s}\Delta l \tag{9}$$

Note that the cases shown in Figures 5 and 6 are coincident when $n_s = 1$.

The problem is to calculate the different Δl. When a displacement is straight or there is a linear interpolation (G1), the segment Δl is the distance between the initial and the final points,

$$\Delta l = \sqrt{(x_{i+1} - x_i)^2 + (y_{i+1} - y_i)^2} \tag{10}$$

If the segment is a circumference arc (or any kind of curve), this arc is replaced by a succession of straight segments with a chordal error e (Figure 10).

$$\Delta\alpha = 2\cos^{-1}\left(1 - \frac{e}{R}\right) \tag{11}$$

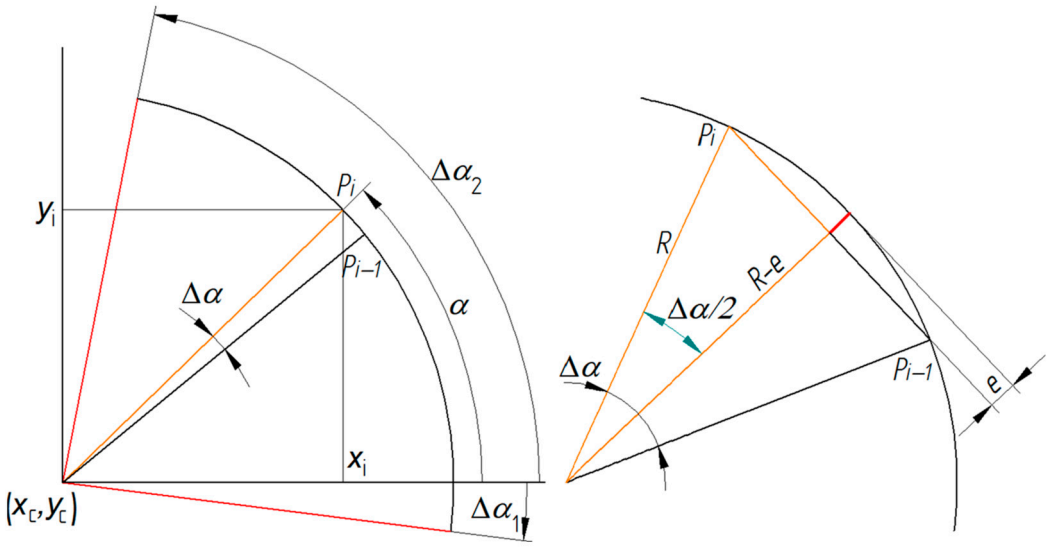

Figure 10. Error produced when the arc is replaced by the chord.

Each arc is divided into segments, such that if the arc goes from an initial angle, α_1, to a final one, α_2, the position (x, y) of the interpolation points can be calculated, obtaining the number of arc segments by rounding up, according to Equation (12):

$$n = ROUNDUP\left(\frac{\alpha_2 - \alpha_1}{\Delta\alpha}, 0\right) \tag{12}$$

The new angle increment is

$$\Delta\alpha = \frac{\alpha_2 - \alpha_1}{n} \tag{13}$$

Applying the last one in order to iterate n times the recursive function, where the first value of α is α_1, the last one is α_2 and the coordinates of any point are

$$\begin{aligned} x_i &= x_c + R\cos\alpha \\ y_i &= y_c + R\sin\alpha \\ \alpha &= \alpha + \Delta\alpha \end{aligned} \tag{14}$$

The rectilinear segment in the XY plane must also be discretised in shorter elements. This is a similar problem, as shown in Figure 11.

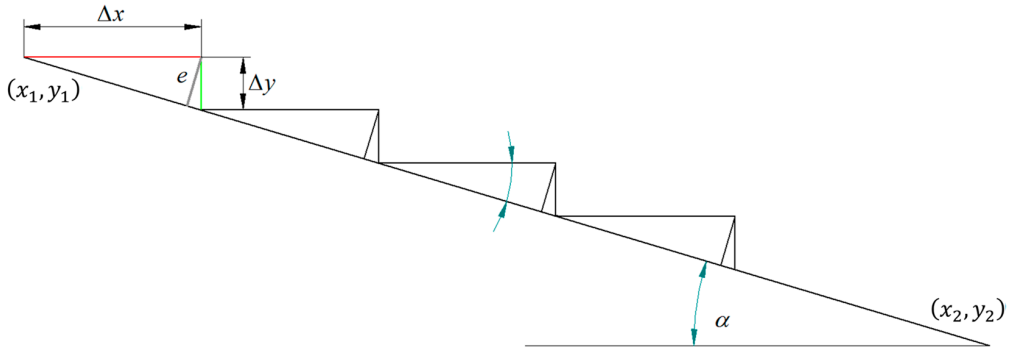

Figure 11. Error produced by discretising a rectilinear segment in shorter elements.

Even though the modern NC machines do describe toolpaths by "leaps", this similitude is going to be used in order to decompose the segment into points, according to the chordal concept, as shown in Figure 11. In this case,

$$\alpha = \tan^{-1}\left(\frac{y_2 - y_1}{x_2 - x_1}\right) \Rightarrow \begin{aligned} \Delta x &= \tfrac{e}{\sin\alpha} \\ \Delta y &= \tfrac{e}{\cos\alpha} \end{aligned} \tag{15}$$

We must consider the particular case of $x_2 - x_1 = 0$, in which the angle is 90°, and, therefore, $\Delta y = e$ and $\Delta x = 0$.

Similarly to Equation (14),

$$\begin{aligned} x_i &= x_{i-1} + \Delta x \\ y_i &= y_{i-1} + R\sin\alpha \\ \text{From } i = 2 \text{ until } x_i > x_2 \text{ inwhichcase } x_i &= x_2 \ : y_i = y_2 \end{aligned} \tag{16}$$

With the points i and $i + 1$, Equation (10) is applied and, after it, Equation (9). For the initial point, the milling tool starts from the first level of Figure 2 and, for each new point, the value of the Equation (9) is increased.

There are two options to achieve the previous objective. The first option would be programming a macro in NC language. The second one would be using an external programming language, for example, with a macro programmed in a spreadsheet. In the first case, the requirement is that the NC machine should calculate the coordinates and process them faster than the machining process occurs, which in old machines (and even in some modern ones) could be difficult when having small chordal errors (Equations (11) and (15)). For this reason, we decided to calculate the coordinates with a Microsoft® Excel® spreadsheet.

3. Practical Implementation

3.1. Simulation

Before the practical test, NC simulation offered an important aid for visualising the trajectory of the milling tool and checking that what was previously programmed with the

spreadsheet macro was exactly what was intended, thus avoiding mistakes and collisions in the real process. For that purpose, the full version of the Fagor™ (Fagor Electrónica, Mondragón, Spain) simulator [30] was used, as described below.

Another advantage is that, if the NC program is going to be run on a machine, with this type of control, we could simulate the use of that machine on our computer. It can be said that the real NC is operated, beyond a mere simulation. Its general interface can be observed in Figure 12.

Figure 12. Graphical interface of the Fagor™ NC simulator.

The simulator has three main areas. The dimensions of the largest one can be customised according to the user's requirements. Thanks to this feature, we defined a main area in order to display the graphical simulation as large as possible, and a secondary area to show the two windows for operating the virtual machine.

The simulation of the program that performs the first contour toolpath is shown in Figure 13. The toolpath described by the centre of the milling tool, on the plate to be milled, can be observed in that figure. Figure 13 also shows the ascending and descending movements.

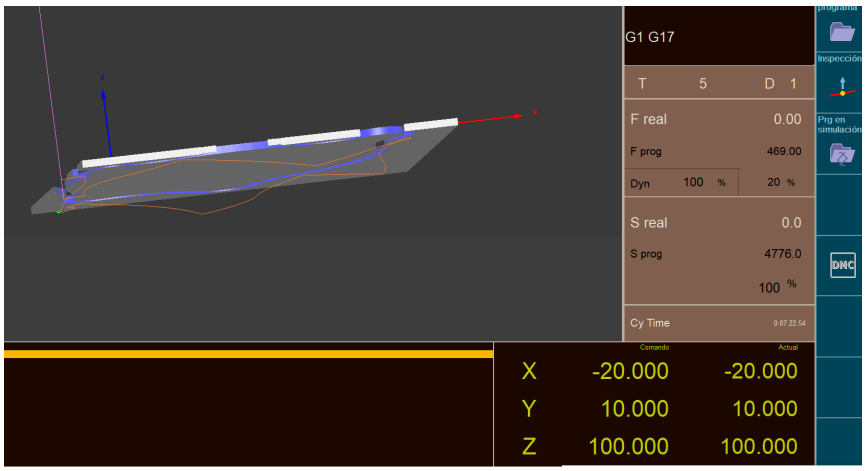

Figure 13. Graphical simulation of the NC program.

This screen is distributed in five areas. The largest one corresponds to the graphics; below it, the programme and the dimensions to be reached can be observed, as well as the distance to them from the current position. In the right area, there are technical parameters and command buttons. Additionally, the two additional windows allow full control of the programme.

Finally, Figure 14 shows the possibility of importing an STL file as raw material or a preform. We used a polyoxymethylene (POM) block into which four threaded holes were drilled. A groove was also milled into the POM block, so that the milling tool could not rub during the process, as checked during the simulation process.

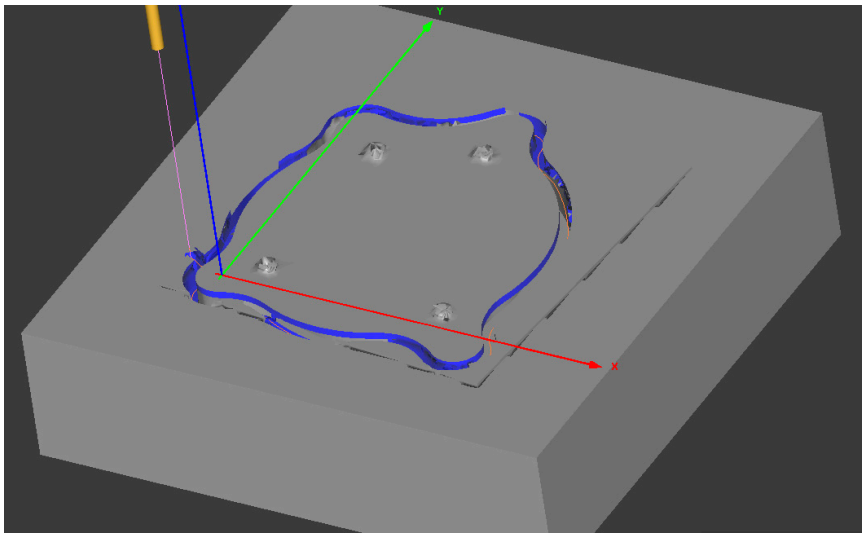

Figure 14. Simulation of the STL file with the preform clamped to the tooling.

The described tooling was clamped in a vice. Thus, removing the screws, the parts could be clamped for the two strategies that were tested during the experimental stage. For the simulation process, it was important to be very careful to draw in the CAD using the same origin that was set in the simulator, so that the part would be correctly positioned in its proper place.

3.2. Materials

The test was performed on a real part, which was a cover in a car engine (Jaguar™, model XK8 (Jaguar, Coventry, UK)), shown in Figure 15. This part has no structural responsibility and it was decided to manufacture it with a titanium alloy (Ti6Al4V), milling a flat plate of 2.7 mm thickness as the original.

The part design was obtained by applying reverse engineering, after scanning it. Two experimental parts were machined, one of them using the method shown in Figure 4, and the second one without vertical displacement. With the first method, uniform wear of the milling tool was expected in all its length. With the second method, the expected wear was only down to the depth of the first 2.7 mm of the milling tool, corresponding to the thickness of the working piece.

For both pieces, the selected milling tools had a diameter of 6 mm and four teeth with an asymmetrical spiral. These milling tools were not specific for titanium, it being possible to use them with a cutting speed of 30 m/min and a feed per tooth of 0.021 mm/tooth, as shown in Figure 16 and as recommended in the manufacturer's catalogue, available online [21]. However, to increase wear in the experimental process, the cutting speed was increased to 60 m/min (previous experiments produced nonappreciable wear after machining over 2 metres with a cutting speed of 30 m/min). We used coolant at 5%.

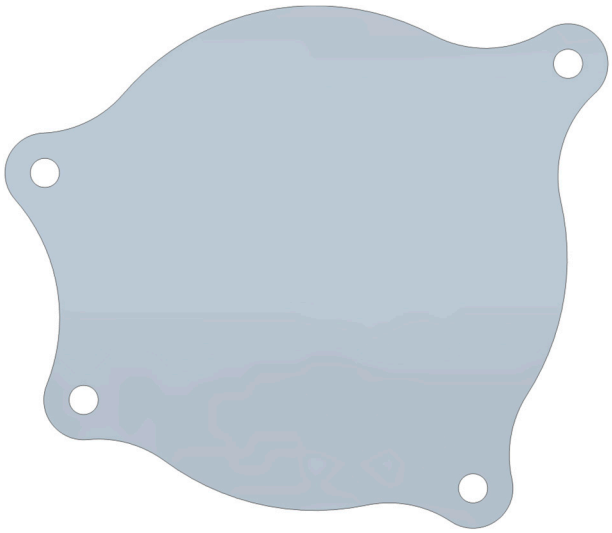

Figure 15. Shape of the experimental part.

Figure 16. Carbide milling tool MA911, with a diameter of 6 mm and a cutting length of 13 mm (12 mm was used), and AlCrN coating.

The first tests were carried out on a three-axes milling machine with a Fagor™ 8070 (Fagor Electrónica, Mondragón, Spain) NC (Figure 17), placed at the CPIFP Corona de Aragón (Vocational Training Centre). The clamping fixture was made at the Centro de Innovación para la Formación Profesional de Aragón, using a similar machine, but with a SIEMENS™ (Siemens, Plano, TX, USA) NC.

Figure 17. Milling machine used for the preliminary tests (**left**) and for making the clamping fixture (**right**).

The final tests were carried out at the facilities of Marena, S.L. (La Puebla de Alfindén, Spain), which is a local company dedicated to the manufacture of cutting tools, using a LAGUN™ (Lagun Machine Tools, Azkoitia, Spain) machine with a FANUC™ (FANUC Iberia, S.L.U., Castelldefels, Spain) NC (Figure 18).

Figure 18. Milling machine used for the final test series.

The expected results should show that the proposed method is better for workshops focused on repairing and maintenance (requiring very small series of parts) than the conventional milling strategy of moving the tool only horizontally.

It should be noted that a general-purpose milling tool was used (specific tools for titanium were intentionally avoided, so that the experimental conditions would be more exigent), as the aim was to simulate a single-part manufacturing process, such as is encountered in maintenance operations, using only the commonly available standard milling tools.

3.3. Practical Test

During the experimental stage, we started (during the preliminary tests) with very conservative machining conditions (cutting speed = 30 m/min and feed rate = 0.021 mm/toot). For this reason, after milling the parts with different strategies, the tools did not show appreciable wear differences on their cutting edges. Thus, it was decided to increase the milled distance, making a total of five helical passes, with a total machined toolpath length of 2321 mm (Figure 19), which is much longer than the 502 mm milled in the preliminary experiments.

Even so, there were no measurable wear differences on the cutting edges of the milling tools. For this reason, it was decided to use less conservative working conditions, i.e., a cutting speed of 60 m/min and feed rate of 0.021 mm/tooth. Obviously, the duration of the milling tool was going to decrease exponentially, as predicted by the Taylor equation, with the coefficients given by Lee and Yoon [31]—Equation (17):

$$v \cdot T^n = C, \quad n = 0.2428 \tag{17}$$

This was then applied to the two cutting speed conditions, as

$$\left.\begin{array}{l} 30 \cdot {T_1}^{0.2428} = C \\ 60 \cdot {T_2}^{0.2428} = C \end{array}\right\rangle \Rightarrow T_2 = 0.06 \cdot T_1 \tag{18}$$

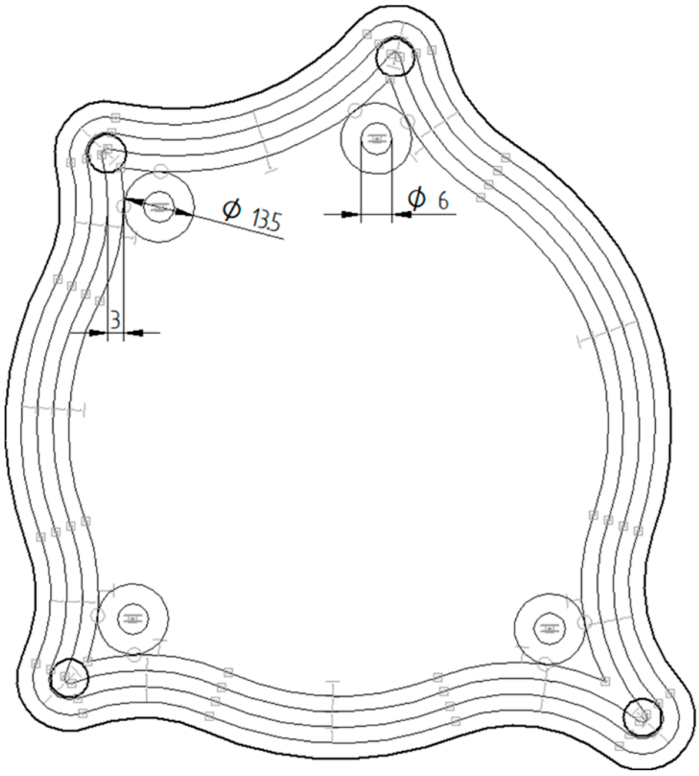

Figure 19. Total milling toolpath, with 5 helical passes.

In other words, it could be expected that the tool would last for a much shorter time, only 6% of the time reached with the previous conservative conditions, so we expected to observe measurable tool wear, as finally happened. For this reason, the workpiece with a flat movement was made in sections, and the wear was measured after each section. The part with helical movement was constructed all in a row, after observing the previously obtained wear results. In the end, the same five contours as in Figure 19 were made, for a total of 2321 mm. Table 1 shows the cutting conditions that were finally chosen.

Table 1. Cutting conditions (coolant at 5%).

Diameter of the milling tool	6 mm
Number of teeth	4 teeth
Used cutting length	12 mm
a_e first run	6 mm
a_e following runs	3 mm
a_z	0.021 mm/tooth
v_c	60 m/min
Total milled length	2321 mm

4. Results and Discussion

Figure 20 shows the measuring equipment (optical inspection machine: Zoller™ (ZOLLER Ibérica S. L., Barcelona, Spain) pomBasicMicro™) that was used to check the wear on the cutting edge of the milling tool, while Figure 21 shows a comparison of the wear that was observed in the milling tools used for both processes.

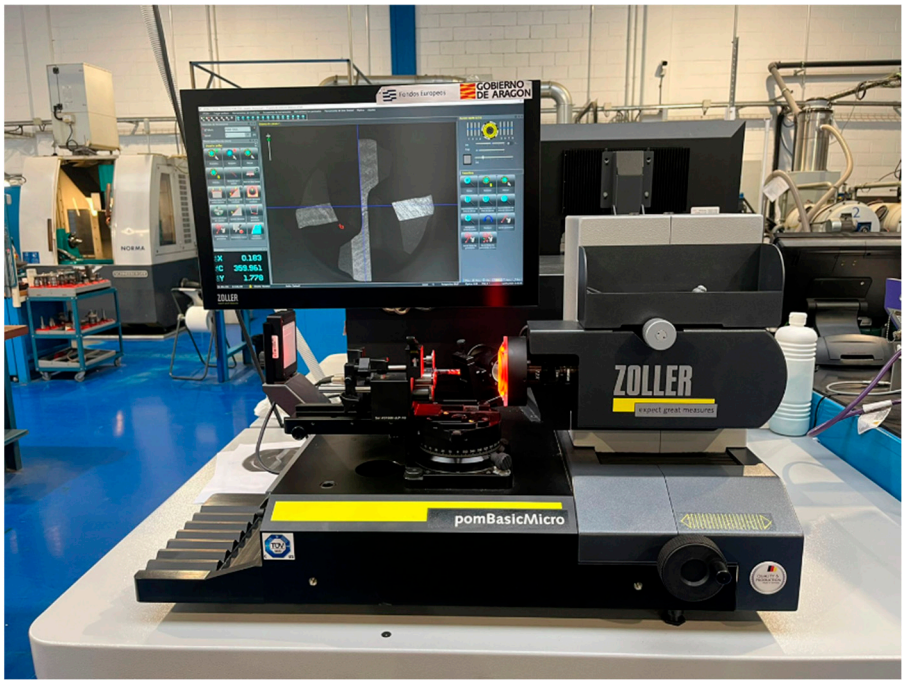

Figure 20. Optical inspection machine used to measure the wear in the milling tools.

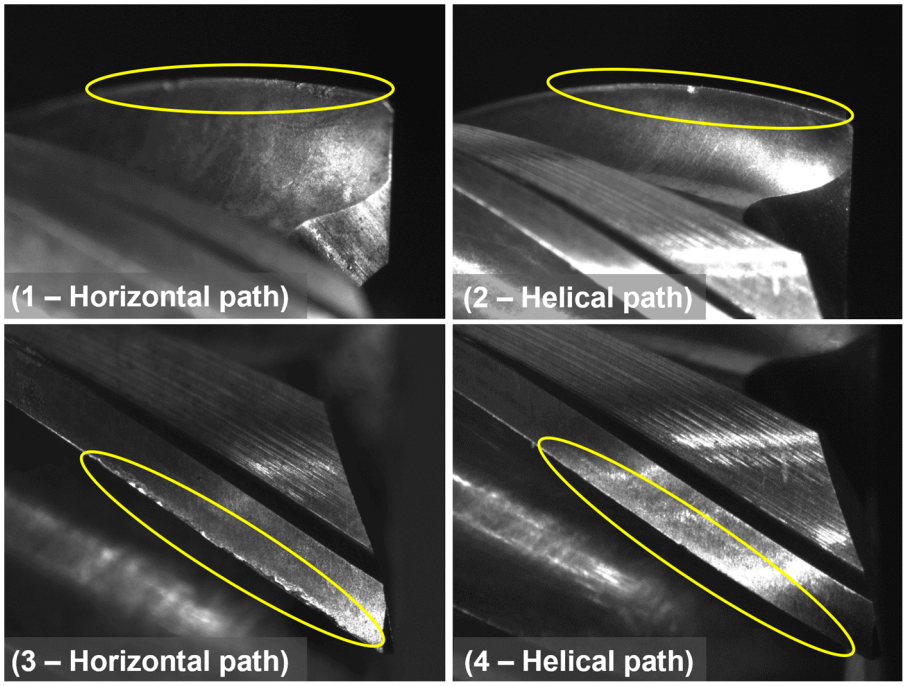

Figure 21. Wear on the cutting edges of the milling tools after the whole milling operation.

4.1. Results

As can be seen, the wear of the milling tool that did not move vertically is much higher than that of the milling tool that did move vertically. The last one shows uniform wear along the entire length of the cutting edge, and it can be used for other milling operations. The milling cutter that was only worn in one area could be used, but its cutting edge already had non-uniform wear that limited its use. Figure 21 is briefly explained below:

(1—Horizontal toolpath)—This is the face of the milling tool that followed a 2D toolpath, in the *XY* plane. Some pitting can be seen in the cutting edge.

(2—Helical toolpath)—This is the face of the milling tool that followed a 3D helical toolpath. The observed wear is very uniform in this case (except for a shiny spot).

(3—Horizontal toolpath)—This is the flank of the milling tool that followed a 2D toolpath, in the *XY* plane. The previously mentioned (1) pitting and wear can be observed on the flank.

(4—Helical toolpath)—This is the flank of the milling tool that followed a 3D helical toolpath. It is not possible to observe significant wear.

Using the full cutting length of the milling tool, uniform wear was produced, which contributed to increasing its service life and, therefore, improved its sustainability in the milling processes (delaying the change of the milling tool and avoiding its premature re-sharpening). In addition, as indicated in [23], it reduced the forces involved, decreasing the required energy consumption.

There is a disadvantage with this method—it can only be applied to the milling of parts without closed-bottom profiles, such that the vertical movement of the milling tool is allowed, while contour milling is performed (milling tools without front sharpening can be used).

4.2. Discussion

The applied method, used on a part with a totally curved shape, could also be applied to other geometries requiring 2D or 3D toolpaths. The most important aspect is to mill plates with thicknesses smaller than the cutting length.

One of the parameters to be optimised could be the half-step (Figures 5 and 8). Although, in our experiments, we preferred to make a helical toolpath, i.e., to distribute the length of the milling tool over the entire perimeter, it would be necessary to consider the length of the half-step (for example, proportional to the diameter of the milling tool). This would be the optimal half-step, although for small perimeters we suggest using only one helical toolpath (Figures 4 and 7). The ascending and descending toolpath generated a contour with the pattern shown in Figure 6c.

However, once the goal of utilising the entire length of the milling tool has been achieved (which would avoid the need to change that tool in the middle of a profiling process, and limit its uniform wear), the influence of the described vertical movement must be studied. This movement alters the helix angle, decreasing it during the downward movement and increasing it during the upward movement, by the value of the slope angle, as shown in Figure 7, Figure 8, and Figure 11. The influence of the helix angle is studied in Reference [32], but the "knife effect" obtained with this new movement can alter the cutting force result, which, as shown in [33], decreases, and will consequently result in a reduction in the consumed energy. Studying the advantages or disadvantages of following a "straight" or "sinusoidal" toolpath (or other toolpaths) is also another possibility for further improvement.

The fact that this process can be used in closed-bottom profiles could also be a line of further research, as the front edge of the cutter would be used not only to finish the bottom, but also to remove material (down milling), due to the downward vertical movement. We are considering implementing this method in pocket milling.

According to the current state of the art, we have found no CAM software that could perform this type of milling. Nevertheless, the 2D or even 3D NC program generated by the CAM software can be processed with the following spreadsheet. Figure 22 shows the input/output data, providing the succession of points (x, y, z) that were transformed to adapt to the Fagor™ 8070 NC and the FANUC™ NC, only containing G1 commands. However, it is essential to use the G5 function or the high-speed functions in order to avoid the marks (Figure 6a), due to the acceleration and deceleration required to reach the position of the described toolpath.

	A	B	C	D	E	F	G	H	I
1	Milling cutter radius, r =	3	mm		X	Y	Z	F	;3D NC line
2	Milling cutting length, l_c =	12	mm		-11.793	5.471	-3.7	335	G1 G5 X-11.793 Y5.471 Z
3	Chamfer or rounding of the mill, c_h =	0.5	mm		-11.611	5.87182	-3.7073		X-11.611 Y5.872 Z-3.707
4	Piece thickness, t_h =	3.2	mm		-11.437	6.27577	-3.7146		X-11.437 Y6.276 Z-3.715
5	Chordal error, e =	0.001	mm		-11.269	6.68273	-3.7218		X-11.269 Y6.683 Z-3.722
6	Milling half-pitch (0 is one helix), p_h =	0	mm		-11.109	7.09258	-3.7291		X-11.109 Y7.093 Z-3.729
7	Starting position (X, Y) =	(-20, 10)			-10.956	7.50518	-3.7364		X-10.956 Y7.505 Z-3.736
8	Vertical milling cutter displacement, l_{cd} =	8.3	mm		-10.81	7.92042	-3.7437		X-10.81 Y7.92 Z-3.744
9	Number of half-pitch =	1			-10.672	8.33816	-3.7509		X-10.672 Y8.338 Z-3.751
10	π =	3.14159265	-0.641418	-0.4356513	-10.541	8.75826	-3.7582		X-10.541 Y8.758 Z-3.758
11	Atan2(C; D) =	2.70722394	-11.793	5.471	-10.417	9.18062	-3.7655		X-10.417 Y9.181 Z-3.766
12	Acos(C) =	0.01240346	0.99992308		-10.301	9.60508	-3.7728		X-10.301 Y9.605 Z-3.773
13	Rounding up (C)=	96	95.8523036		-10.192	10.0315	-3.7801		X-10.192 Y10.032 Z-3.78
14	Rounding (C) =	5.402	5.40242044		-10.091	10.4598	-3.7873		X-10.091 Y10.46 Z-3.787
15	Perimeter 2D =	501.85802	Pitagoras		-9.9973	10.8898	-3.7946		X-9.997 Y10.89 Z-3.795
16	Perimeter 3D =	501.920399	501.926651		-9.9113	11.3214	-3.8019		X-9.911 Y11.321 Z-3.802
17	G1 X-11.793 Y5.471 F381 S4776 M3; (1)	Length of the section			-9.8328	11.7544	-3.8092		X-9.833 Y11.754 Z-3.809
18	G3 X-11.053 Y24.747 I-22.678 J10.522; (2)	19.8036919	19.8036919		-9.7621	12.1888	-3.8165		X-9.762 Y12.189 Z-3.816
19	G2 X-7.616 Y78.815 I62.056 J23.198; (3)	55.8129056	75.6165975		-9.6989	12.6243	-3.8237		X-9.699 Y12.624 Z-3.824
20	G3 X-5.512 Y96.646 I-22.12 J11.649; (4)	18.3646587	93.9812562		-9.6435	13.0609	-3.831		X-9.643 Y13.061 Z-3.831
21	G2 X10.052Y112.517 I12.596 J3.214; (5)	26.6615999	120.642856		-9.5957	13.4983	-3.8383		X-9.596 Y13.498 Z-3.838
22	G3 X51.857 Y126.457 I9.591 J40.89; (6)	46.3899383	167.032794		-9.5556	13.9366	-3.8456		X-9.556 Y13.937 Z-3.846
23	G2 X74.58 Y120.637 I9.971 J-8.342; (7)	29.2464411	196.279235		-9.5233	14.3755	-3.8528		X-9.523 Y14.375 Z-3.853
24	G3 X85.927 Y104.242 I24.525 J4.85; (8)	20.5088429	216.788078		-9.4987	14.8149	-3.8601		X-9.499 Y14.815 Z-3.86
25	G2 X113.551 Y26.111 I-34.924 J-56.297; (9)	89.5298118	306.31789		-9.4818	15.2546	-3.8674		X-9.482 Y15.255 Z-3.867
26	G3 X118.482 Y1.249 I23.603 J-8.239; (10)	26.5809334	332.898824		-9.4727	15.6946	-3.8747		X-9.473 Y15.695 Z-3.875
27	G2 X100.553 Y-17.467 I-9.71 J-8.644; (11)	38.7743287	371.673152		-9.4713	16.1347	-3.882		X-9.471 Y16.135 Z-3.882
28	G3 X75.502 Y-13.608 I-15.807 J-19.369; (12)	26.5812463	398.254399		-9.4777	16.5747	-3.8892		X-9.478 Y16.575 Z-3.889
29	G2 X24.018 Y-12.56 I-24.499 J61.554; (13)	52.8876694	451.142068		-9.4918	17.0146	-3.8965		X-9.492 Y17.015 Z-3.897
30	G3 X4.733 Y-12.108 I-10.183 J-22.832; (14)	19.8040887	470.946157		-9.5136	17.4541	-3.9038		X-9.514 Y17.454 Z-3.904
31	G2 X-11.793 Y5.471 I-4.733 J12.108; (1)	30.9118637	501.85802		-9.5432	17.8932	-3.9111		X-9.543 Y17.893 Z-3.911

Figure 22. Input/output data, providing the succession of points in the spreadsheet.

The original NC 2D program was added from row 17, in the first column, although we have preferred to show that it is identical to the 3D program, but without the Z-coordinates.

Finally, the obtained results emphasise the importance of applying the toolpath model in order to completely use the full length of the milling tool flutes, when it is possible, and also to perform a previous simulation of the process. These two aspects can reduce the costs associated with tool wearing and re-sharpening. Thanks to this, the service life of the tool can be improved in many processes of air-contour milling.

5. Conclusions

The intended goal of using almost the entire length of the milling tool was achieved. The only condition for this was that the part must be bottomless (or the bottom is far enough from the milling tool) in what we have termed processes of "air-contour milling".

This method makes possible several improvements in the process:

- The longer life of the milling tool edges, increasing the number of parts to be milled before they get worn;
- Uniform wear of the milling tool edges along their entire length, instead of local wear areas. This allows one to distribute the wear of the edges;
- The possibility of working with general-purpose milling tools, instead of using more expensive specialised ones;
- Increasing the sustainability of the milling processes, thanks to the optimisation of the milling tool's life, as the entire cutting edge is used, instead of having to discard it due to wear concentration in one area.

In short, the improvements in the geometry of the milling tools and the milling toolpaths, under the same cutting conditions, increase the life of these milling tools, reducing the process times, which results in an increase in the process's sustainability.

The disadvantage of this method is that it is only applicable to processes of air-contour milling, without a bottom or where the milling tool does not use its front teeth.

The aforementioned disadvantage will make it possible to develop further research considering the following two aspects:

- Trying to apply this method to parts with a bottom, in processes such as pocket milling, which would imply the use of front teeth;
- Analysing the use of milling tools without front teeth, for processes of air-contour milling, which would reduce their manufacturing costs.

Author Contributions: Conceptualization, C.G.-H., J.-L.H.-T., P.U.-A. and J.-J.V.-S.; methodology, C.G.-H., M.G.-A., J.-L.H.-T. and J.-J.V.-S.; software, J.-L.H.-T. and J.-J.V.-S.; validation, C.G.-H., J.-J.G.-B., M.G.-A., J.-L.H.-T., F.V.-C. and J.-J.V.-S.; formal analysis, C.G.-H. and J.-L.H.-T.; investigation, C.G.-H., J.-L.H.-T., P.U.-A. and J.-J.V.-S.; resources, J.-J.G.-B.; M.G.-A., J.-L.H.-T. and F.V.-C.; data curation, C.G.-H. and J.-L.H.-T.; writing—original draft preparation, C.G.-H., J.-J.V.-S. and J.-L.H.-T.; writing—review and editing, A.T., C.G.-H., P.U.-A., J.-L.H.-T. and J.-J.V.-S.; supervision, A.T., C.G.-H., M.G.-A. and J.-L.H.-T. All authors have read and agreed to the published version of the manuscript.

Funding: This research received funding from the Government of Aragon's *Departamento de Ciencia, Universidad y Sociedad del Conocimiento*, through the research group Design for Safety (D4S), with the reference: T70_23D (period 2023-2025).

Data Availability Statement: The original data presented in this study are openly available in Zenodo: https://doi.org/10.5281/zenodo.14974310.

Acknowledgments: The authors want to thank the following: *CPIFP Corona de Aragón* (Vocational Training Centre), where the preliminary tests were carried out. *Centro de Innovación para la Formación Profesional de Aragón* (Centre for Innovation in Vocational Training in Aragón), where the clamping fixture was made. Finally, we would like to thank Marena, S.L., where the final tests were carried out and the wear of the tools was measured.

Conflicts of Interest: Mariano García-Arbués was employed by Marena, S.L. Co., Ltd. The remaining author declare that the research was conducted in the absence of any commercial or financial relationships that could be construed as a potential conflict of interest.

References

1. Guo, L.; Yang, W.; Sun, J. A Continuous Oscillating Milling Strategy Based on Uniform Wear Theory for Improving the Service Life of the Ball-End Cutter. *Tribol. Int.* **2024**, *192*, 109318. [CrossRef]
2. Guo, L.; Liao, X.; Yang, W.; Sun, J. An Oscillating Milling Strategy Based on the Uniform Wear Theory for Improving Service Life of the Ball-End Cutter. *J. Mater. Process. Technol.* **2023**, *317*, 117993. [CrossRef]
3. Luo, M.; Luo, H.; Zhang, D.; Tang, K. Improving Tool Life in Multi-Axis Milling of Ni-Based Superalloy with Ball-End Cutter Based on the Active Cutting Edge Shift Strategy. *J. Mater. Process. Technol.* **2018**, *252*, 105–115. [CrossRef]
4. Villarrazo, N.; Sáinz De La Maza, Á.; Caneda, S.; Bai, L.; Pereira, O.; López De Lacalle, L.N. Effect of Tool Orientation on Surface Roughness and Dimensional Accuracy in Ball End Milling of Thin-Walled Blades. *Int. J. Adv. Manuf. Technol.* **2025**, *136*, 383–395. [CrossRef]
5. Käsemodel, R.B.; de Souza, A.F.; Voigt, R.; Basso, I.; Rodrigues, A.R. CAD/CAM Interfaced Algorithm Reduces Cutting Force, Roughness, and Machining Time in Free-Form Milling. *Int. J. Adv. Manuf. Technol.* **2020**, *107*, 1883–1900. [CrossRef]
6. Vavruska, P.; Bartos, F.; Stejskal, M.; Pesice, M.; Zeman, P.; Heinrich, P. Increasing Tool Life and Machining Performance by Dynamic Spindle Speed Control along Toolpaths for Milling Complex Shape Parts. *J. Manuf. Process.* **2023**, *99*, 283–297. [CrossRef]
7. Zhang, X.F.; Xie, J.; Xie, H.F.; Li, L.H. Experimental Investigation on Various Tool Path Strategies Influencing Surface Quality and Form Accuracy of CNC Milled Complex Freeform Surface. *Int. J. Adv. Manuf. Technol.* **2012**, *59*, 647–654. [CrossRef]
8. Garde Barace, J.-J.; Huertas-Talón, J.-L.; Valdivia Calvo, F.; Bueno-Pérez, J.-A.; Cano-Álvarez, B.; Alcázar-Sánchez, M.-Á.; Ponz-Cuenca, R.; Tzotzis, A. Velocidad de Corte Constante En Fresado. *IMHE* **2021**, *476*, 100–115.
9. Conradie, P.; Oosthuizen, T.; Dimitrov, D.; Saxer, M. Effect of Milling Strategy and tool geometry on machining cost when cutting titanium alloys. *S. Afr. J. Ind. Eng.* **2015**, *26*, 137–151. [CrossRef]
10. García-Hernández, C.; Garde-Barace, J.-J.; Valdivia-Sánchez, J.-J.; Ubieto-Artur, P.; Bueno-Pérez, J.-A.; Cano-Álvarez, B.; Alcázar-Sánchez, M.-Á.; Valdivia-Calvo, F.; Ponz-Cuenca, R.; Huertas-Talón, J.-L.; et al. Trochoidal Milling Path with Variable Feed. Application to the Machining of a Ti-6Al-4V Part. *Mathematics* **2021**, *9*, 2701. [CrossRef]

11. Jacso, A.; Szalay, T.; Sikarwar, B.S.; Phanden, R.K.; Singh, R.K.; Ramkumar, J. Investigation of Conventional and ANN-Based Feed Rate Scheduling Methods in Trochoidal Milling with Cutting Force and Acceleration Constraints. *Int. J. Adv. Manuf. Technol.* **2023**, *127*, 487–506. [CrossRef]
12. Minquiz, G.M.; Meraz-Melo, M.A.; Flores Méndez, J.; González-Sierra, N.E.; Munoz-Hernandez, G.A.; Piñón Reyes, A.C.; Moreno Moreno, M. Sustainable Assessment of a Milling Manufacturing Process Based on Economic Tool Life and Energy Modeling. *J. Braz. Soc. Mech. Sci. Eng.* **2023**, *45*, 365. [CrossRef]
13. Singh, K.; Sultan, I.A. A Computer-Aided Sustainable Modelling and Optimization Analysis of CNC Milling and Turning Processes. *J. Manuf. Mater. Process.* **2018**, *2*, 65. [CrossRef]
14. Bhat, P.; Agrawal, C.; Khanna, N. Development of a Sustainability Assessment Algorithm and Its Validation Using Case Studies on Cryogenic Machining. *J. Manuf. Mater. Process.* **2020**, *4*, 42. [CrossRef]
15. Mehmood, T.; Khalil, M.S. Enhancement of Machining Performance of Ti-6Al-4V Alloy Though Nanoparticle-Based Minimum Quantity Lubrication: Insights into Surface Roughness, Material Removal Rate, Temperature, and Tool Wear. *J. Manuf. Mater. Process.* **2024**, *8*, 293. [CrossRef]
16. García-Hernández, C.; Martínez-Angulo, A.; Efkolidis, N.; Ubieto-Artur, P.; Huertas-Talón, J.L.; Kyratsis, P. Applying High Speed Video to Optimize the Performance of Milling Tools. In Proceedings of the Advances on Mechanics, Design Engineering and Manufacturing II; Cavas-Martínez, F., Eynard, B., Fernández Cañavate, F.J., Fernández-Pacheco, D.G., Morer, P., Nigrelli, V., Eds.; Springer: New York, NY, USA, 2019; pp. 422–429.
17. Tima, T.S.; Geier, N. Machining-Induced Burr Suppression in Edge Trimming of Carbon Fibre-Reinforced Polymer (CFRP) Composites by Tool Tilting. *J. Manuf. Mater. Process.* **2024**, *8*, 247. [CrossRef]
18. Krajnik, P.; Kopač, J. Modern Machining of Die and Mold Tools. *J. Mater. Process. Technol.* **2004**, *157–158*, 543–552. [CrossRef]
19. Vavruska, P.; Pesice, M.; Zeman, P.; Kozlok, T. Automated Feed Rate Optimization with Consideration of Angular Velocity According to Workpiece Shape. *Results Eng.* **2022**, *16*, 100762. [CrossRef]
20. Vavruska, P.; Bartos, F.; Pesice, M. Effective Feed Rate Control to Maintain Constant Feed per Tooth along Toolpaths for Milling Complex–Shaped Parts. *Int. J. Adv. Manuf. Technol.* **2023**, *128*, 3215–3232. [CrossRef]
21. Marena, S.L. Website. Available online: https://marena.es/ (accessed on 26 February 2025).
22. Puerta-Morales, F.J.; Gomez, J.S.; Fernandez-Vidal, S.R. Study of the Influence of Helical Milling Parameters on the Quality of Holes in the UNS R56400 Alloy. *Appl. Sci.* **2020**, *10*, 845. [CrossRef]
23. Inácio, R.H.; Da Silva, R.H.L.; Pereira, I.C.; Hassui, A. Suppressing Notch Wear by Changing the Tool Path in the Side Milling of a Ti-6Al-4 V Alloy. *Int. J. Adv. Manuf. Technol.* **2023**, *125*, 453–463. [CrossRef]
24. Denkena, B.; Biermann, D. Cutting Edge Geometries. *CIRP Ann.* **2014**, *63*, 631–653. [CrossRef]
25. Uhlmann, E.; Oberschmidt, D.; Löwenstein, A.; Kuche, Y. Influence of Cutting Edge Preparation on the Performance of Micro Milling Tools. *Procedia CIRP* **2016**, *46*, 214–217. [CrossRef]
26. Vavruska, P.; Maly, J.; Novotny, A. Increasing Tool Life through Adjustment of Cutting Edge and Toolpath during Milling of Inconel 718. *MM SJ* **2022**, *2022*, 6283–6288. [CrossRef]
27. Gross, D.; Friedl, F.; Meier, T.; Hanenkamp, N. Comparison of Linear and Trochoidal Milling for Wear and Vibration Reduced Machining. *Procedia CIRP* **2020**, *90*, 563–567. [CrossRef]
28. Yan, G.; Zhang, D.; Xu, J.; Sun, Y. Corner Smoothing for CNC Machining of Linear Tool Path: A Review. *J. Adv. Manuf. Sci. Technol.* **2023**, *3*, 2023001. [CrossRef]
29. Fagor Automation CNCelite 8058/8060/8065/8070 Programming Manual. Available online: https://www.fagorautomation.com/en/downloads (accessed on 1 April 2025).
30. Fagor Free Simulator. Fagor Automation. Available online: https://www.fagorautomation.com/es/documentacion#/descarga/8060-65-70-free-simulator/896496 (accessed on 1 April 2025).
31. Lee, Y.J.; Yoon, H.-S. Modeling of Cutting Tool Life with Power Consumption Using Taylor's Equation. *J. Mech. Sci. Technol.* **2023**, *37*, 3077–3085. [CrossRef]
32. Plodzien, M.; Burek, J.; Zylka, L.; Sulkowicz, P. The Influence of End Mill Helix Angle on High Performance Milling Process. *J. Mech. Sci. Technol.* **2020**, *34*, 817–827. [CrossRef]
33. LopezdeLacalle, L.N.L.; Lamikiz, A.; Sanchez, J.A.; FernandezdeBustos, I.F. Simultaneous Measurement of Forces and Machine Tool Position for Diagnostic of Machining Tests. *IEEE Trans. Instrum. Meas.* **2005**, *54*, 2329–2335. [CrossRef]